Supplementary information

High quality samples of La-substituted $BiFeO_3$ prepared by mechanosynthesis

Antonio Perejón[a,b], Pedro E. Sánchez-Jiménez[a], José M. Criado[a], Luis A. Pérez-Maqueda[a], Julio Romero de Paz[c], Regino Sáez-Puche[d], Nahum Masó[e], Anthony R. West[f]

[a]*Instituto de Ciencia de Materiales de Sevilla (CSIC-Universidad de Sevilla). C. Américo Vespucio 49, Sevilla 41092. Spain*

[b]*Department of Chemistry, Inorganic Chemistry Laboratory, University of Oxford, South Parks Road, Oxford, OX1 3QR, United Kingdom*

[c]*Universidad Complutense de Madrid, CAI Técnicas Físicas, Ciudad Universitaria s/n, Madrid, Spain*

[d]*Departamento Química Inorgánica, Facultad de Ciencias Químicas, Universidad Complutense de Madrid, Ciudad Universitaria, 28040 Madrid, Spain*

[e]*Centre for Material Science and Nanotechnology (SMN) Forskningsparken Gaustadallèen 21 0349 Oslo. Norway*

[f]*Department of Materials Science and Engineering, University of Sheffield, S1 3JD Sheffield, UK*

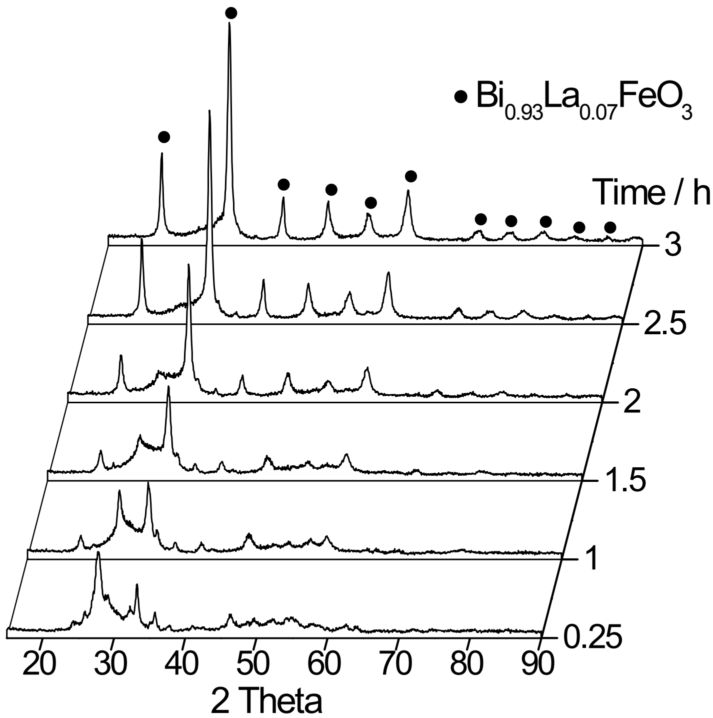

Figure S1. Diffraction patterns at different milling times of the solids obtained after milling under oxygen (7 bar) the stoichiometric amounts of the single oxides necessary for the composition $Bi_{0.93}La_{0.07}FeO_3$.

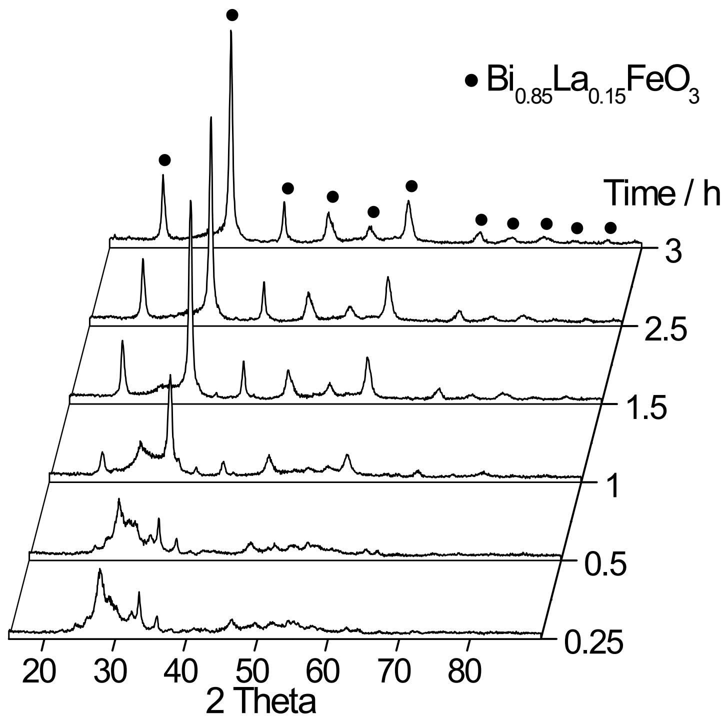

Figure S2. Diffraction patterns at different milling times of the solids obtained after milling under oxygen (7 bar) the stoichiometric amounts of the single oxides necessary for the composition $Bi_{0.85}La_{0.15}FeO_3$.

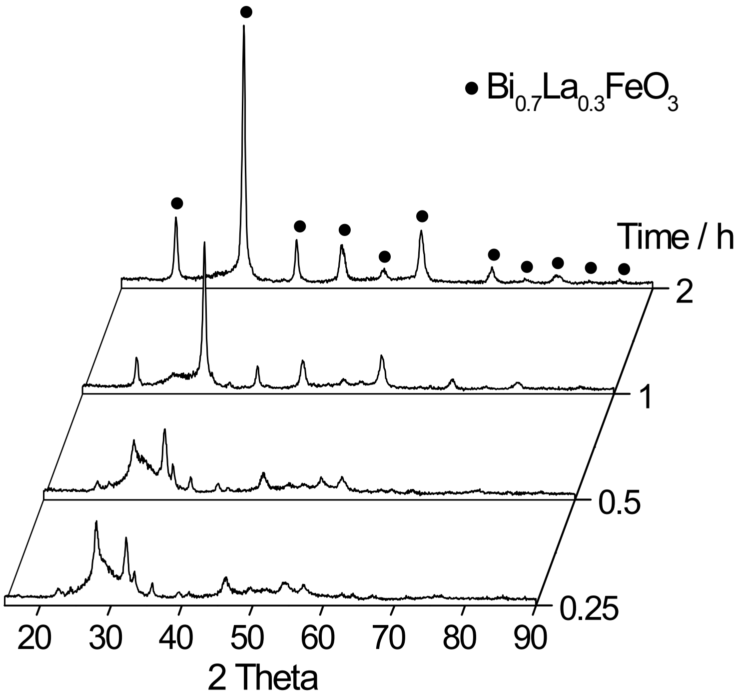

Figure S3. Diffraction patterns at different milling times of the solids obtained after milling under oxygen (7 bar) the stoichiometric amounts of the single oxides necessary for the composition $Bi_{0.70}La_{0.30}FeO_{3.}$

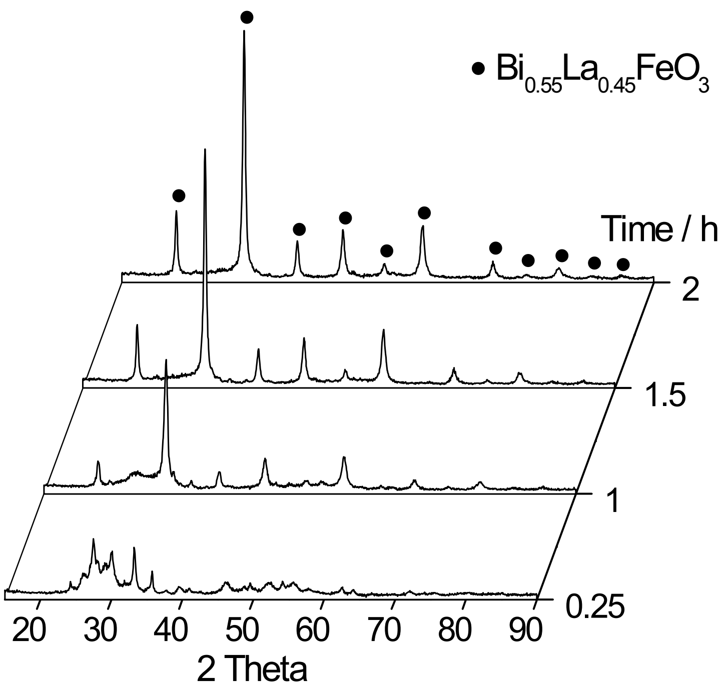

Figure S4. Diffraction patterns at different milling times of the solids obtained after milling under oxygen (7 bar) the stoichiometric amounts of the single oxides necessary for the composition $Bi_{0.55}La_{0.45}FeO_{3.}$

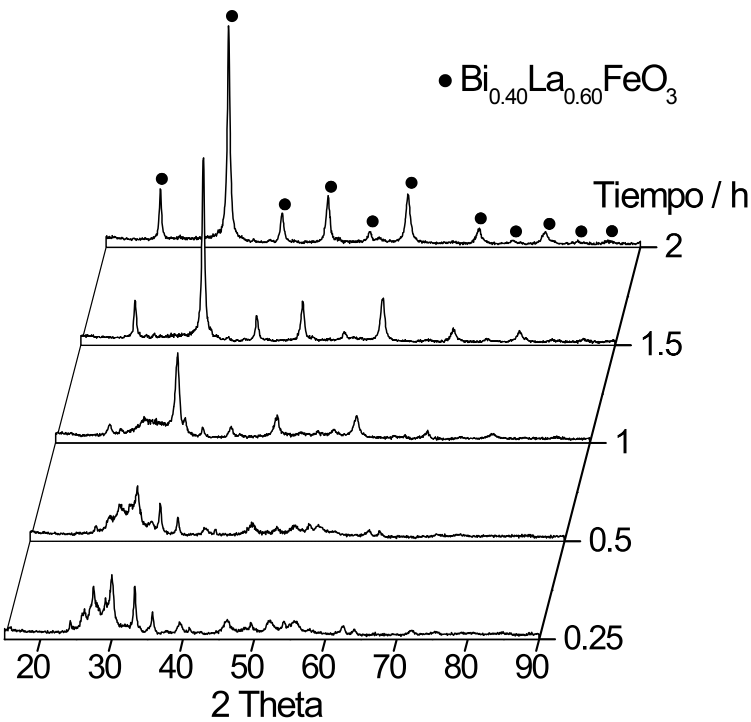

Figure S5. Diffraction patterns at different milling times of the solids obtained after milling under oxygen (7 bar) the stoichiometric amounts of the single oxides necessary for the composition $Bi_{0.40}La_{0.60}FeO_3$.

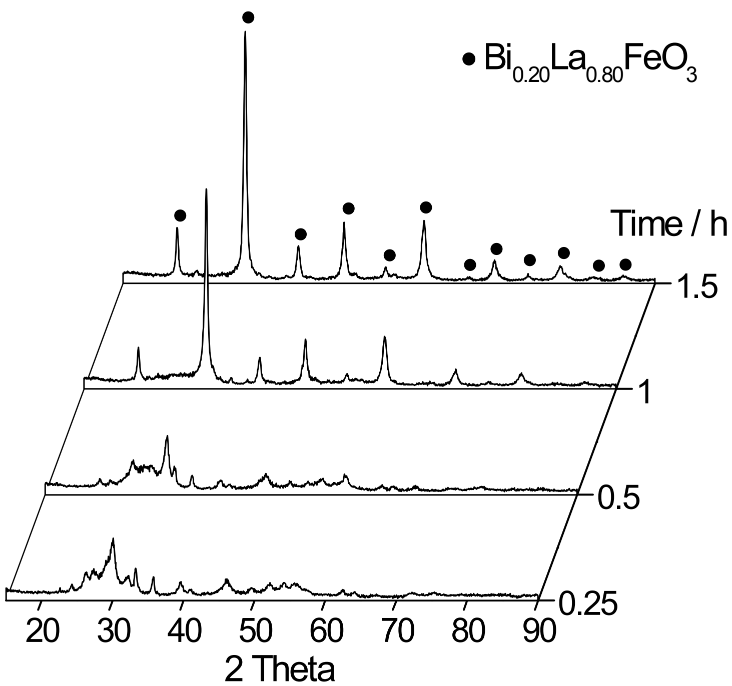

Figure S6. Diffraction patterns at different milling times of the solids obtained after milling under oxygen (7 bar) the stoichiometric amounts of the single oxides necessary for the composition $Bi_{0.20}La_{0.80}FeO_3$.

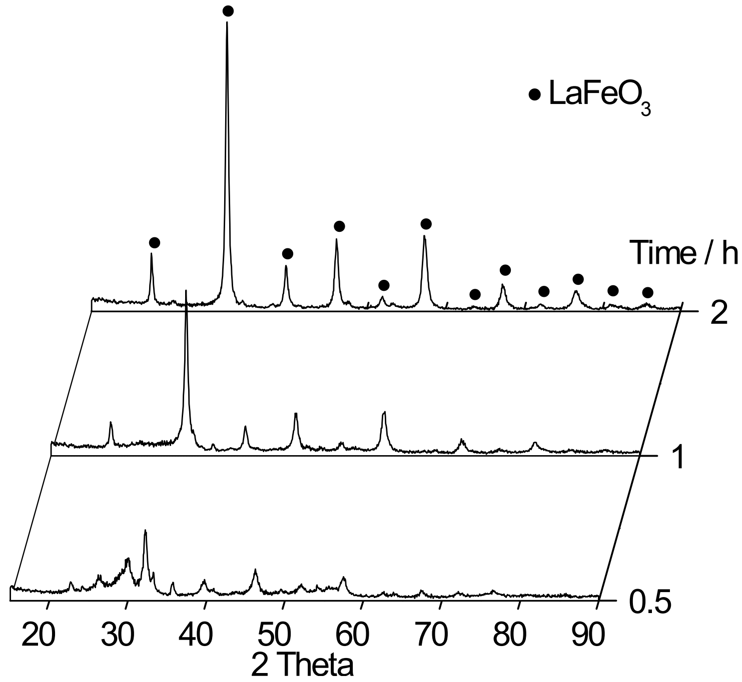

Figure S7. Diffraction patterns at different milling times of the solids obtained after milling under oxygen (7 bar) the stoichiometric amounts of the single oxides necessary for the composition $LaFeO_3$.

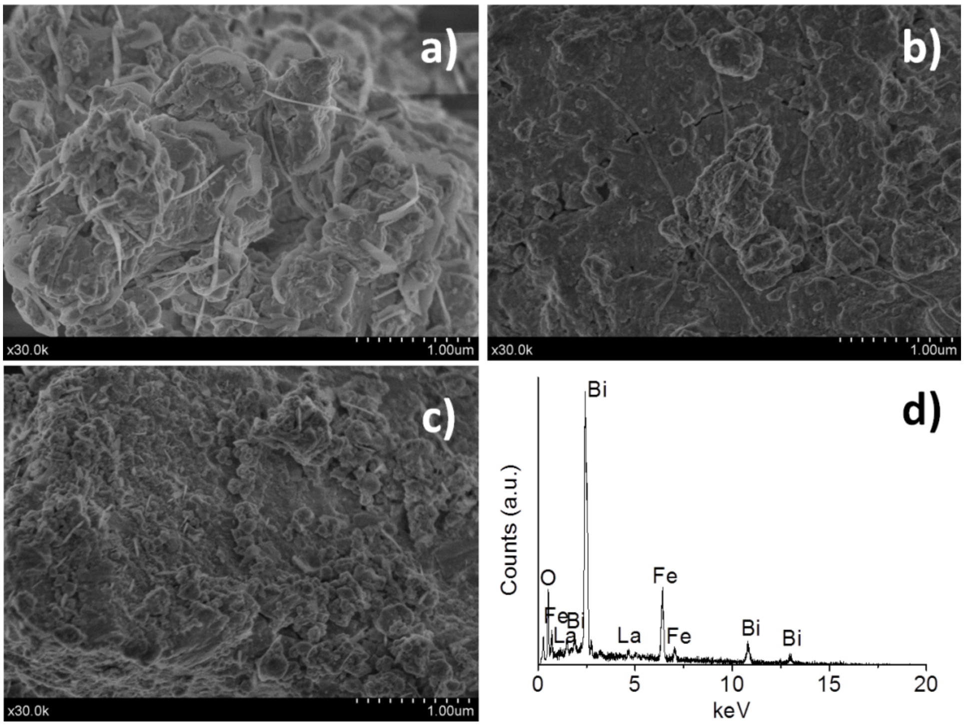

Figure S8. SEM micrographs corresponding to powders obtained after milling the single oxides necessary for the composition $Bi_{0.93}La_{0.07}FeO_3$. Micrographs were taken after milling (a) 0.5 h, (b) 1 h, (c) 3 h, (d) EDX spectrum of the product shown in (c).

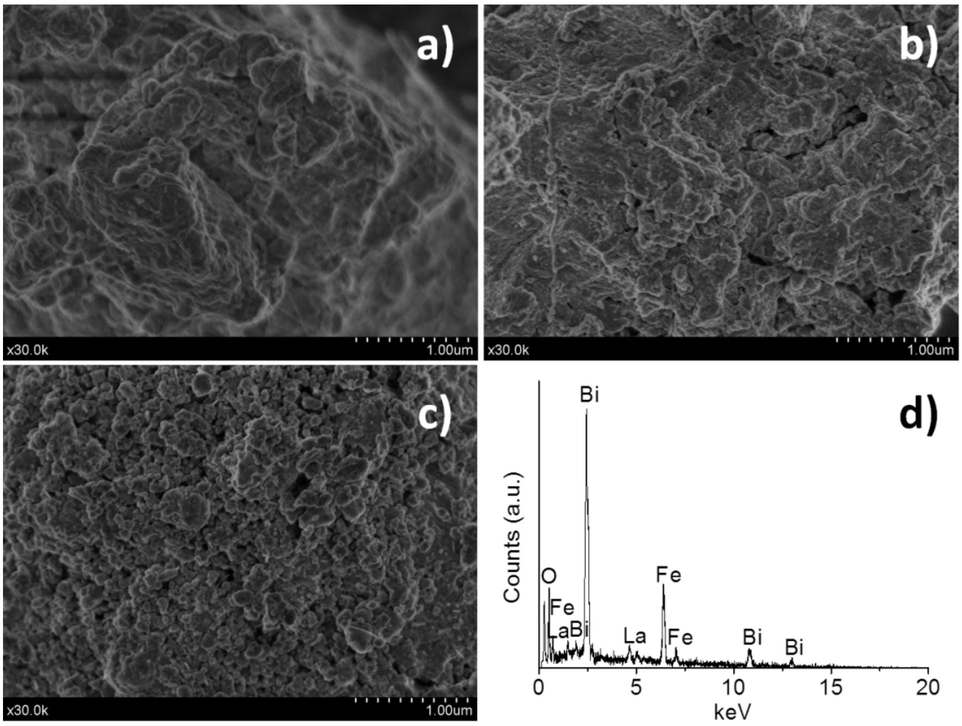

Figure S9. SEM micrographs corresponding to powders obtained after milling the single oxides necessary for the composition $Bi_{0.85}La_{0.15}FeO_3$. Micrographs were taken after milling (a) 0.5 h, (b) 1.5 h, (c) 3 h, (d) EDX spectrum of the product shown in (c).

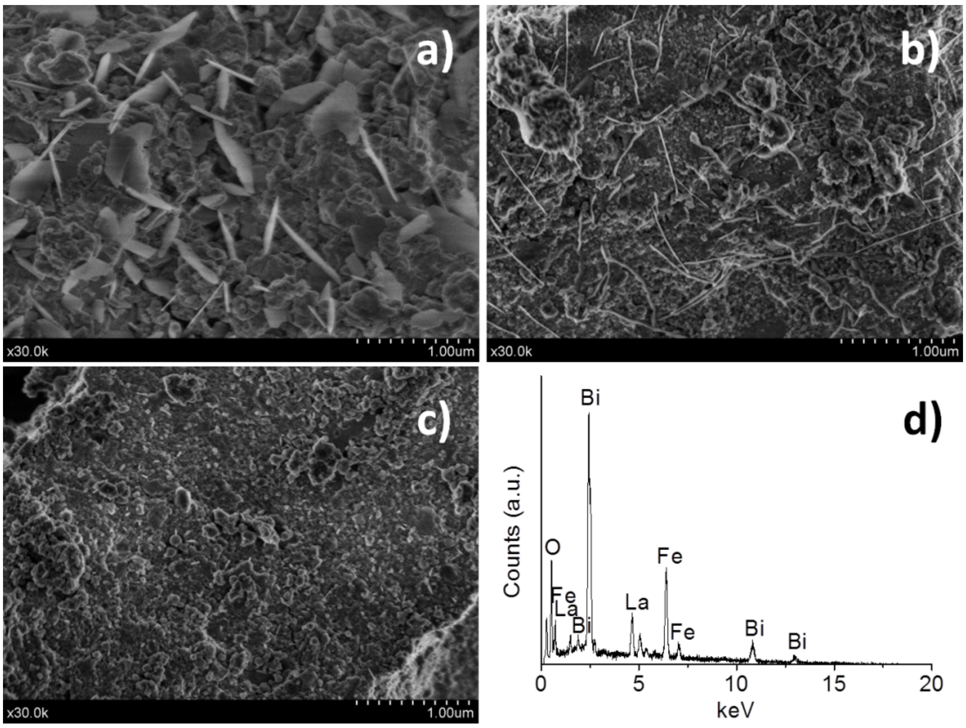

Figure S10. SEM micrographs corresponding to powders obtained after milling the single oxides necessary for the composition $Bi_{0.70}La_{0.30}FeO_3$. Micrographs were taken after milling: (a) 0.25 h, (b) 1 h, (c) 2 h, (d) EDX spectrum of the product shown in (c).

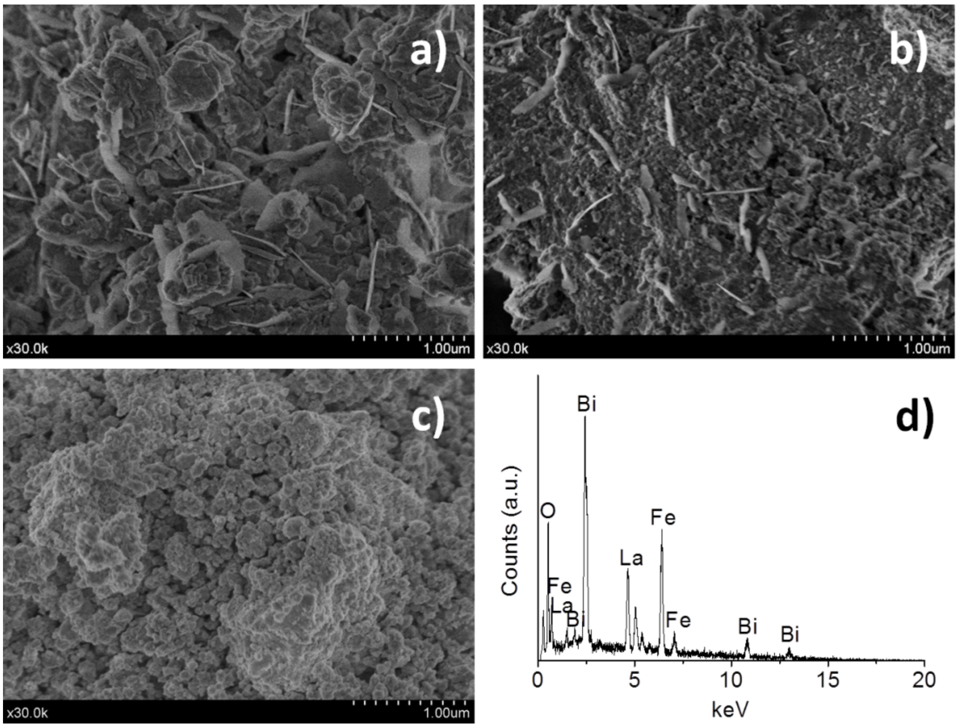

Figure S11. SEM micrographs corresponding to powders obtained after milling the single oxides necessary for the composition $Bi_{0.55}La_{0.45}FeO_3$. Micrographs were taken after milling: (a) 0.5 h, (b) 1 h, (c) 2 h, (d) EDX spectrum of the product shown in (c).

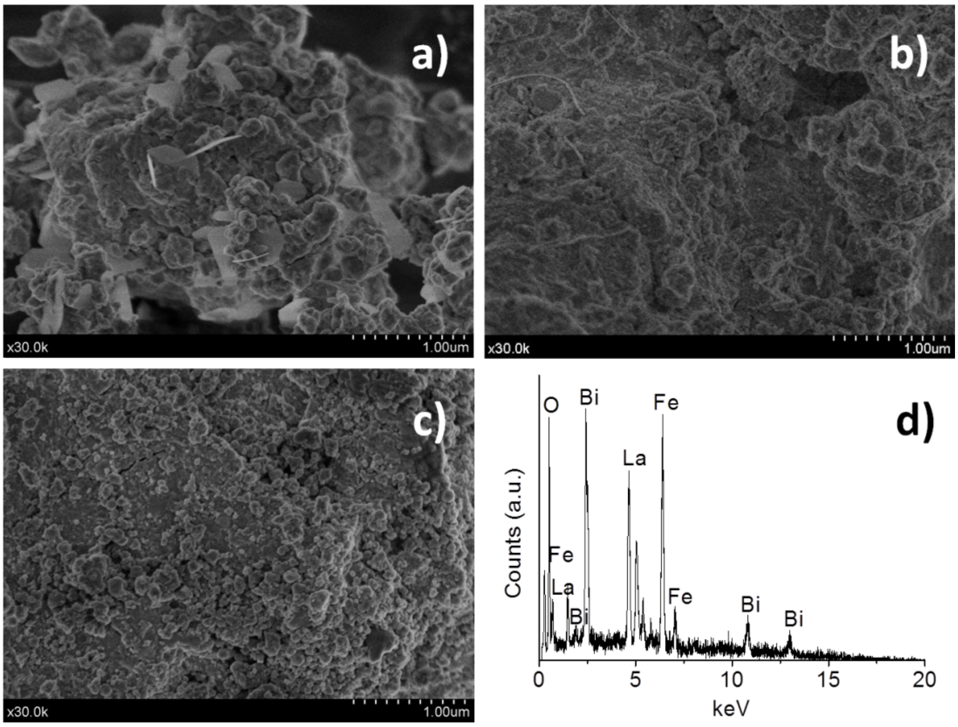

Figure S12. SEM micrographs corresponding to powders obtained after milling the single oxides necessary for the composition $Bi_{0.40}La_{0.60}FeO_3$. Micrographs were taken after milling: (a) 0.5 h, (b) 1 h, (c) 2 h, (d) EDX spectrum of the product shown in (c).

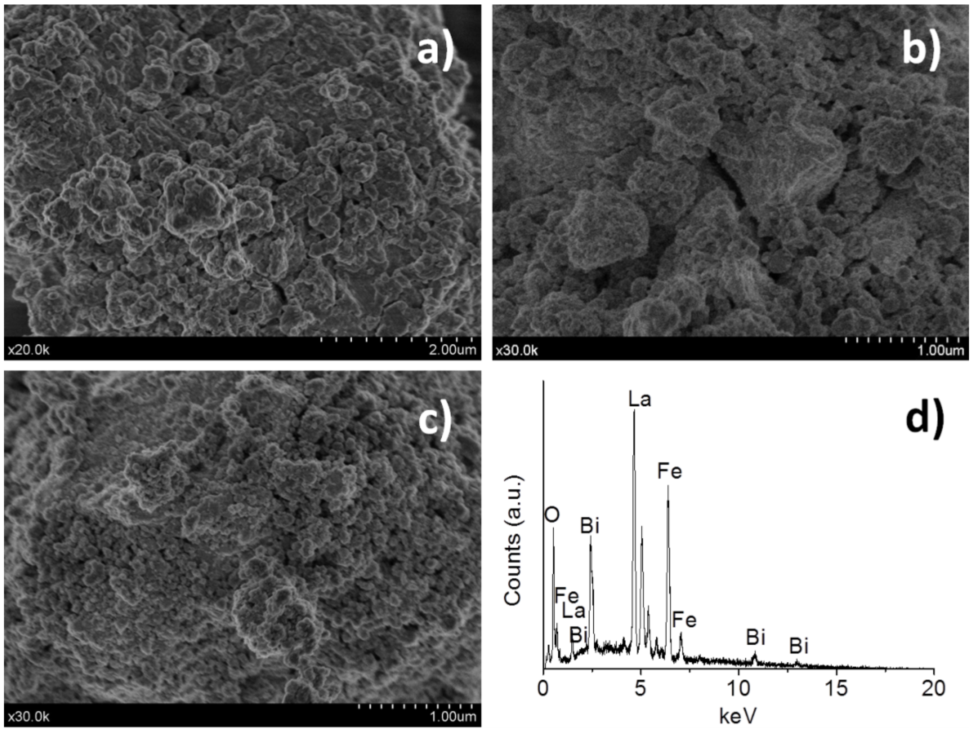

Figure S13. SEM micrographs corresponding to powders obtained after milling the single oxides necessary for the composition $Bi_{0.20}La_{0.80}FeO_3$. Micrographs were taken after milling: (a) 0.25 h, (b) 1 h, (c) 1.5 h, (d) EDX spectrum of the product shown in (c).

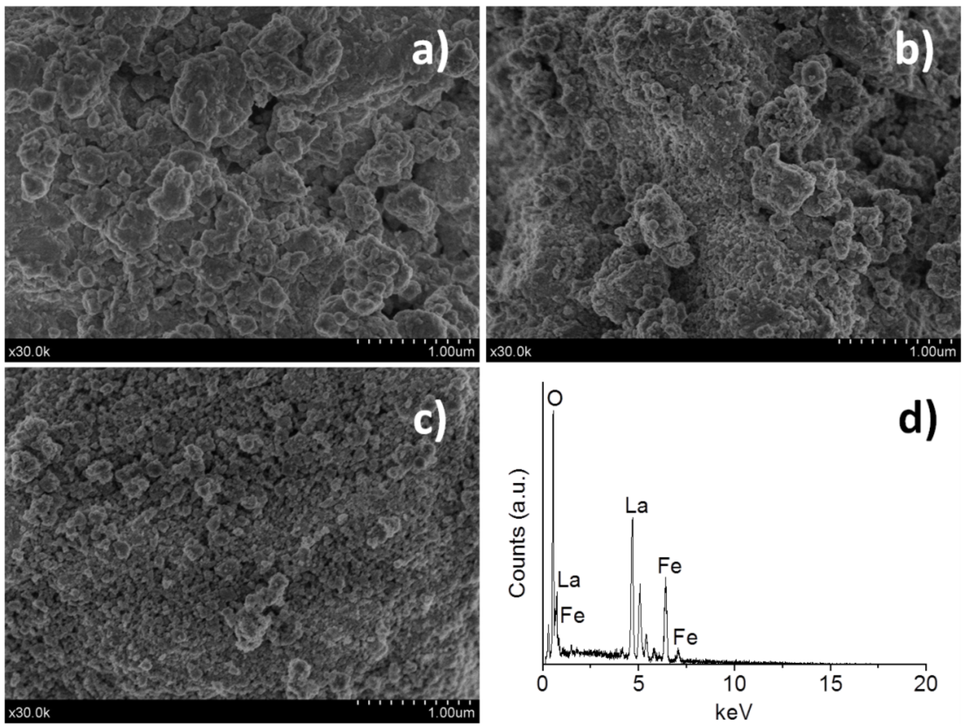

Figure S14. SEM micrographs corresponding to powders obtained after milling the single oxides necessary for the composition $LaFeO_3$. Micrographs were taken after milling: (a) 0.5 h, (b) 1 h, (c) 2 h, (d) EDX spectrum of the product shown in (c).

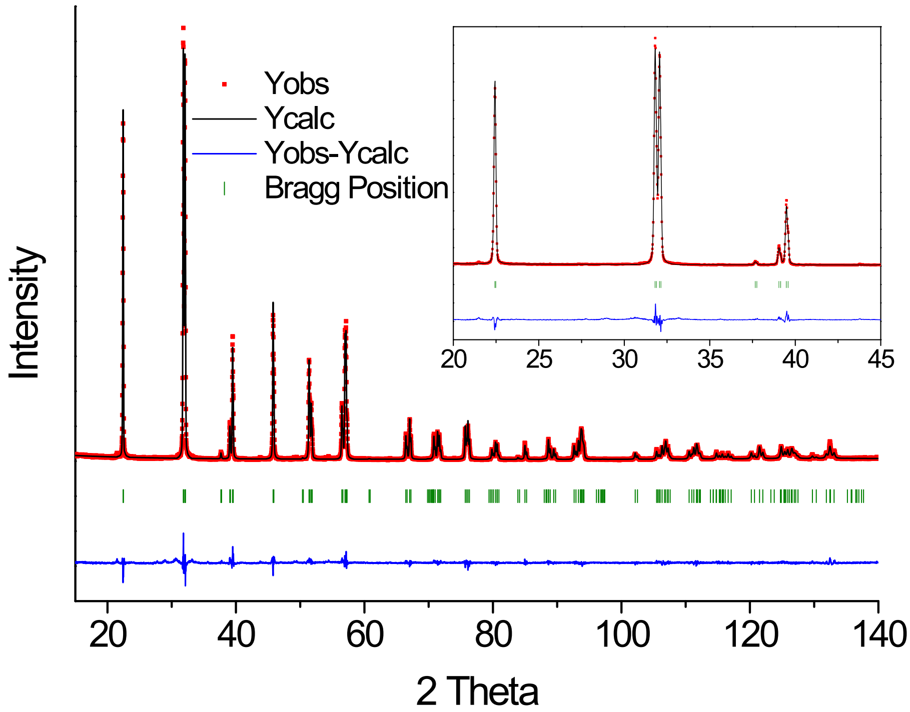

Figure S15. Diffraction pattern corresponding to the sample $Bi_{0.93}La_{0.07}FeO_3$ obtained after milling the single oxides for 3 hours, and heated to 800ºC (dots). The solid lines are the results of the Rietveld refinement. The inset shows a detail of the refinement in the range 20-45º where the maxima peaks are observed.

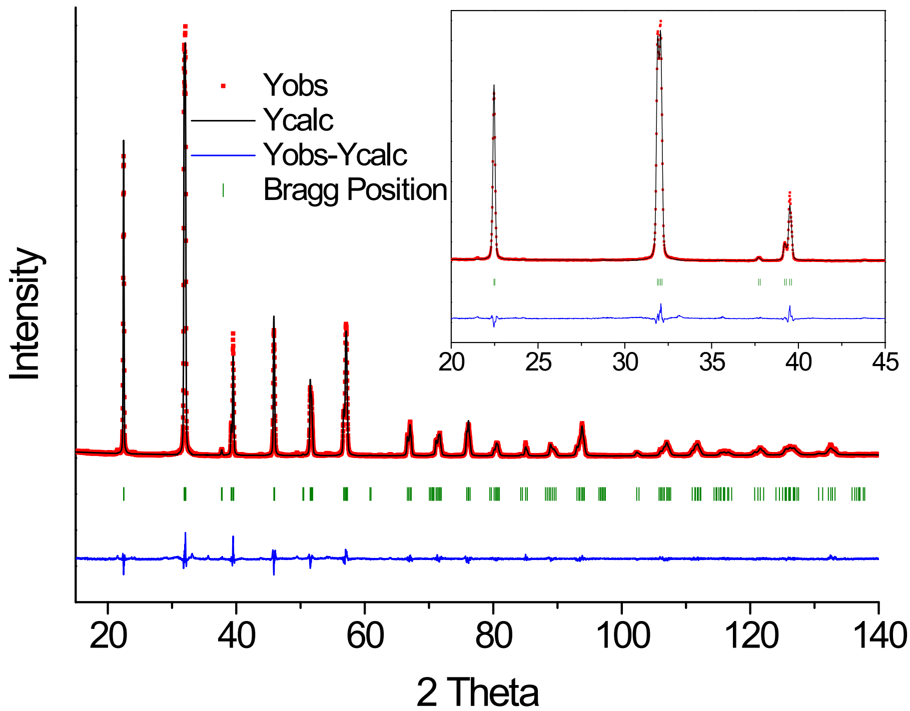

Figure S16. Diffraction pattern corresponding to the sample $Bi_{0.85}La_{0.15}FeO_3$ obtained after milling the single oxides for 3 hours, and heated to 800ºC (dots). The solid lines are the results of the Rietveld refinement. The inset shows a detail of the refinement in the range 20-45º where the maxima peaks are observed.

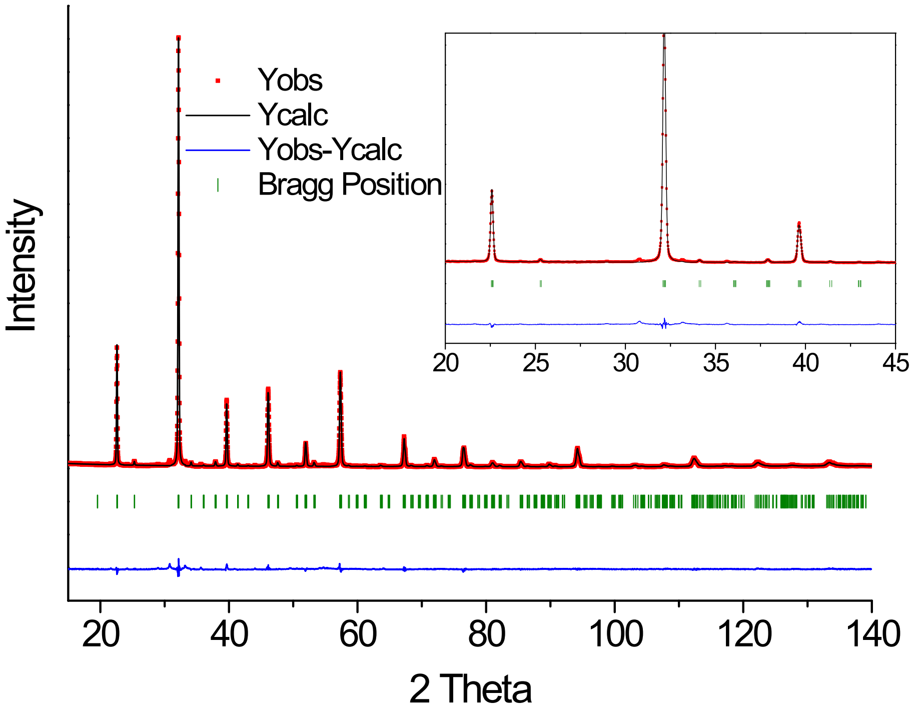

Figure S17. Diffraction pattern corresponding to the sample $Bi_{0.55}La_{0.45}FeO_3$ obtained after milling the single oxides for 2 hours, and heated to 800ºC (dots). The solid lines are the results of the Rietveld refinement. The inset shows a detail of the refinement in the range 20-45º where the maxima peaks are observed.

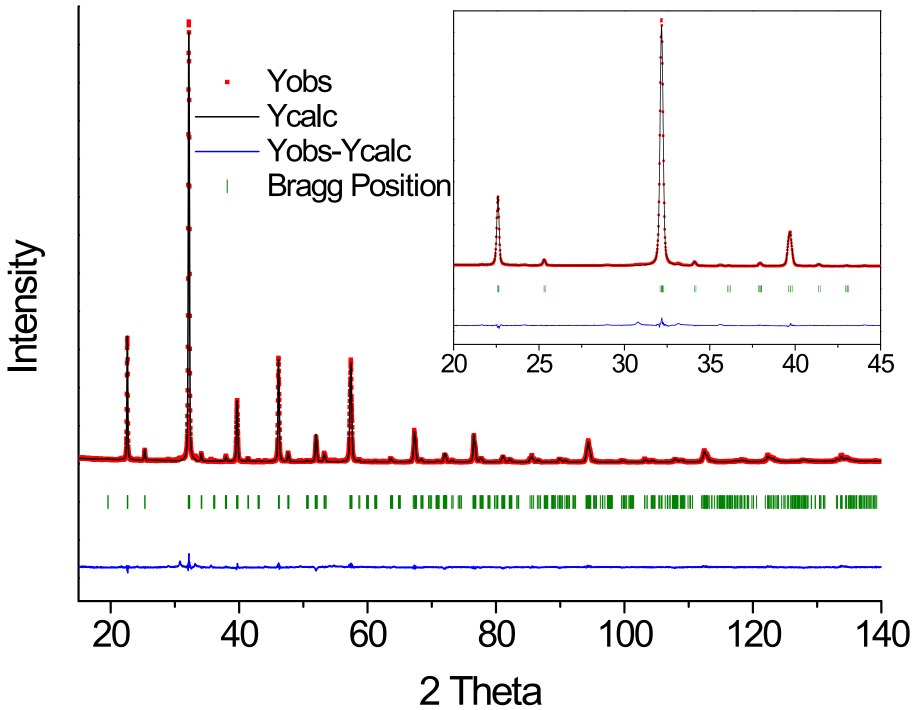

Figure S18. Diffraction pattern corresponding to the sample $Bi_{0.40}La_{0.60}FeO_3$ obtained after milling the single oxides for 2 hours and heated to 800ºC (dots). The solid lines are the results of the Rietveld refinement. The inset shows a detail of the refinement in the range 20-45º where the maxima peaks are observed.

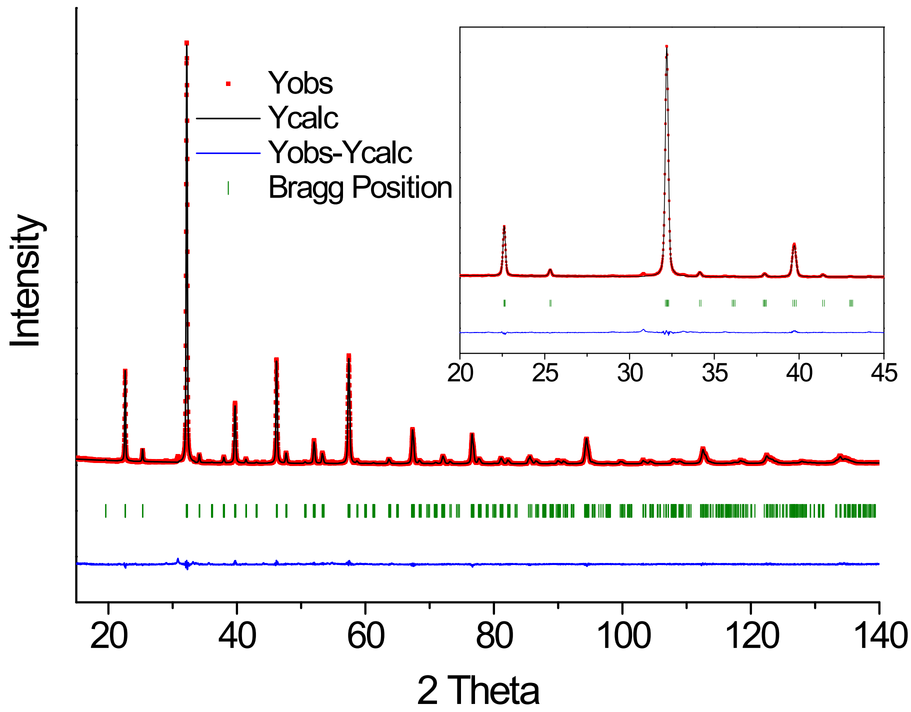

Figure S19. Diffraction pattern corresponding to the sample $Bi_{0.20}La_{0.80}FeO_3$ obtained after milling the single oxides for 2 hours and heated to 800ºC (dots). The solid lines are the results of the Rietveld refinement. The inset shows a detail of the refinement in the range 20-45º where the maxima peaks are observed.

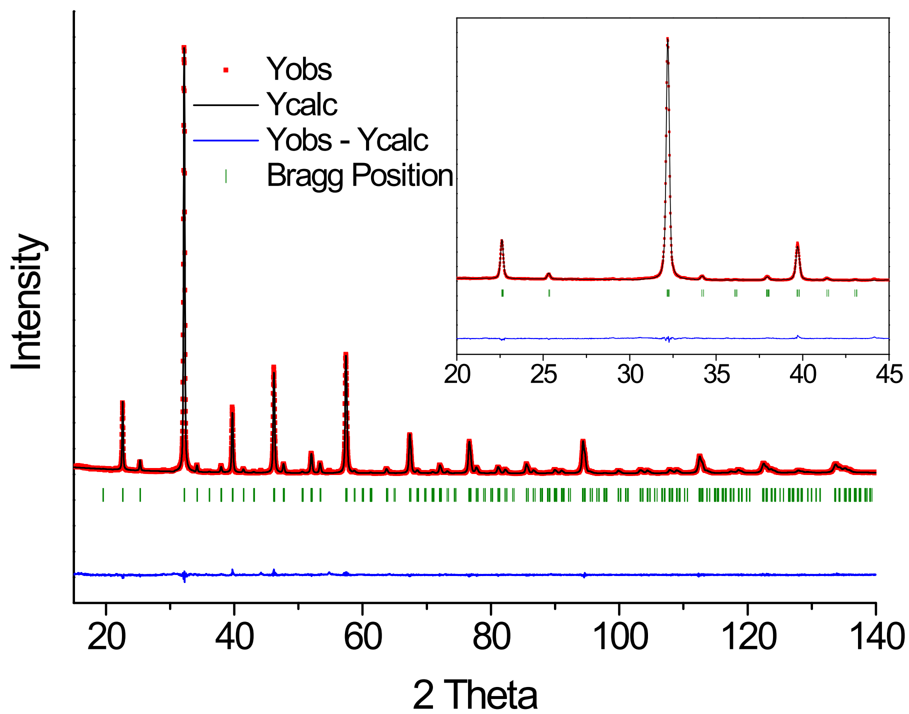

Figure S20. Diffraction pattern corresponding to the sample $LaFeO_3$ obtained after milling the single oxides for 2 hours and heated to 800ºC (dots). The solid lines are the results of the Rietveld refinement. The inset shows a detail of the refinement in the range 20-45º where the maxima peaks are observed.

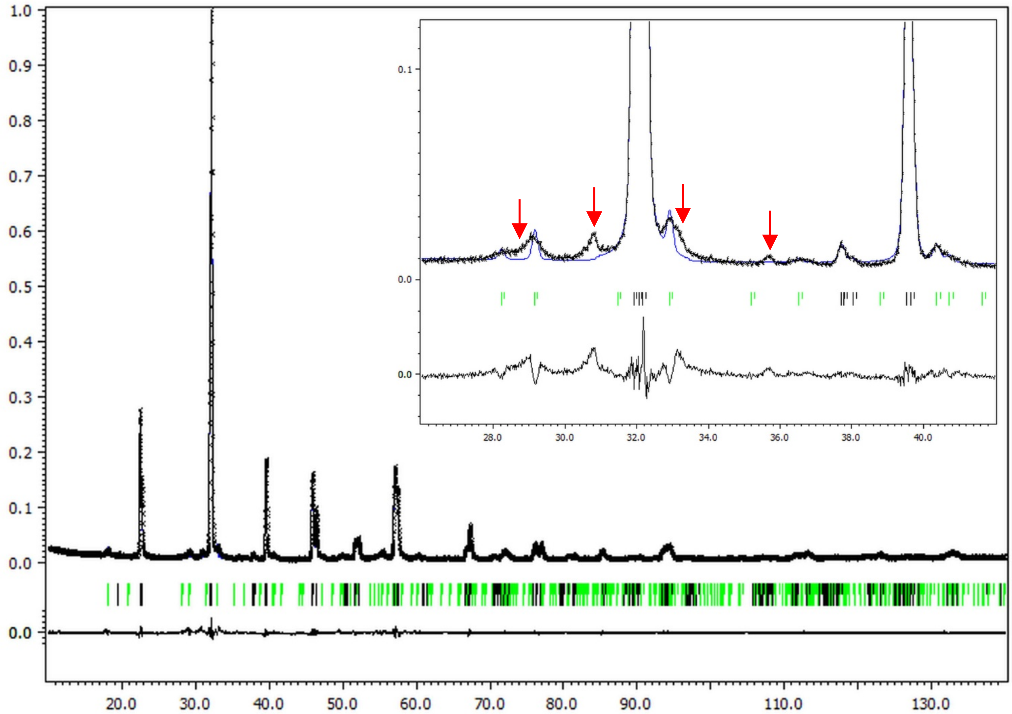

Figure S21. Diffraction pattern corresponding to the sample $Bi_{0.70}La_{0.30}FeO_3$ obtained after milling the single oxides for 2 hours and heated to 800ºC (dots). The refinement of the pattern with Jana2006 in LeBail pattern match mode was performed considering the superspace group Imma(00γ)s00 . The inset shows a detail of the refinement in the range 26-42º. The red arrows indicate the satellite peaks not fitted by this super structure.

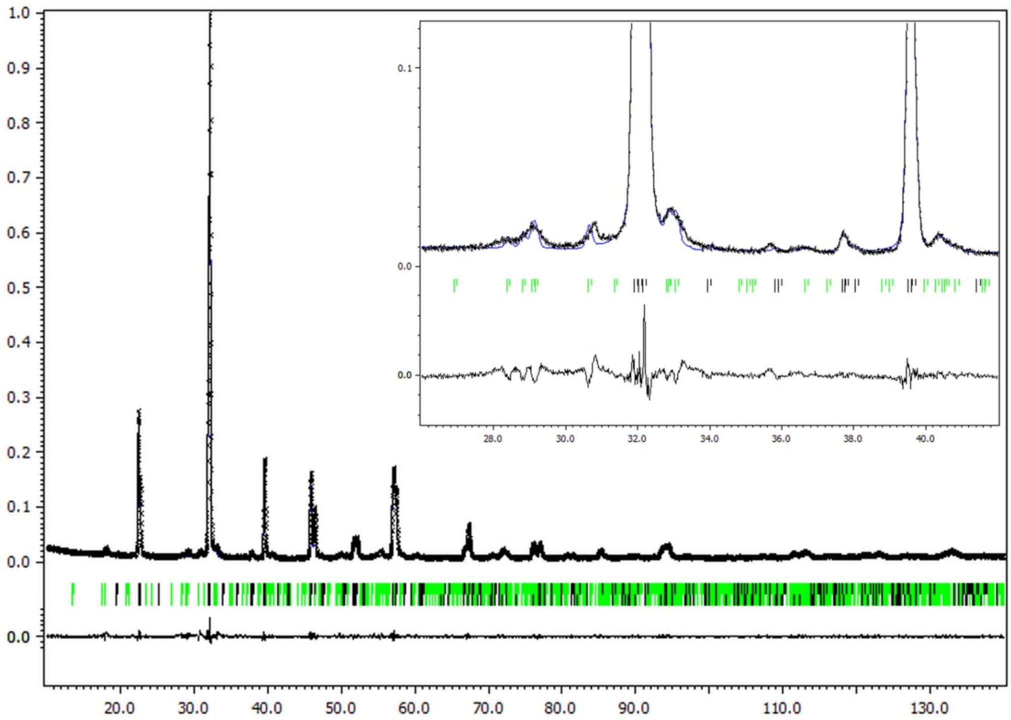

Figure S22. Rietveld refinement of the pattern of the sample $Bi_{0.70}La_{0.30}FeO_3$ with Jana2006 in LeBail pattern match mode considering the superspace group $Pn2_1a(00\gamma)s00$. The inset shows a detail of the refinement in the range 26-42º. All satellite peaks are fitted by this super structure.

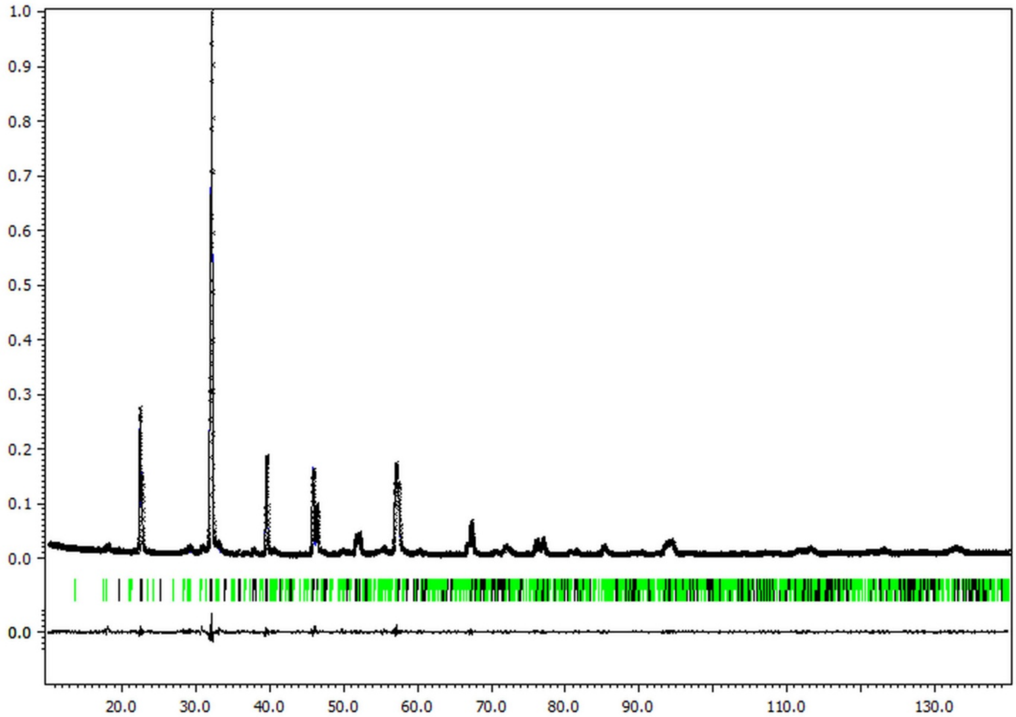

Figure S23. Full Rietveld refinement of the pattern of the sample $Bi_{0.70}La_{0.30}FeO_3$ with Jana2006 considering the superspace group $Pn2_1a(00\gamma)s00$.

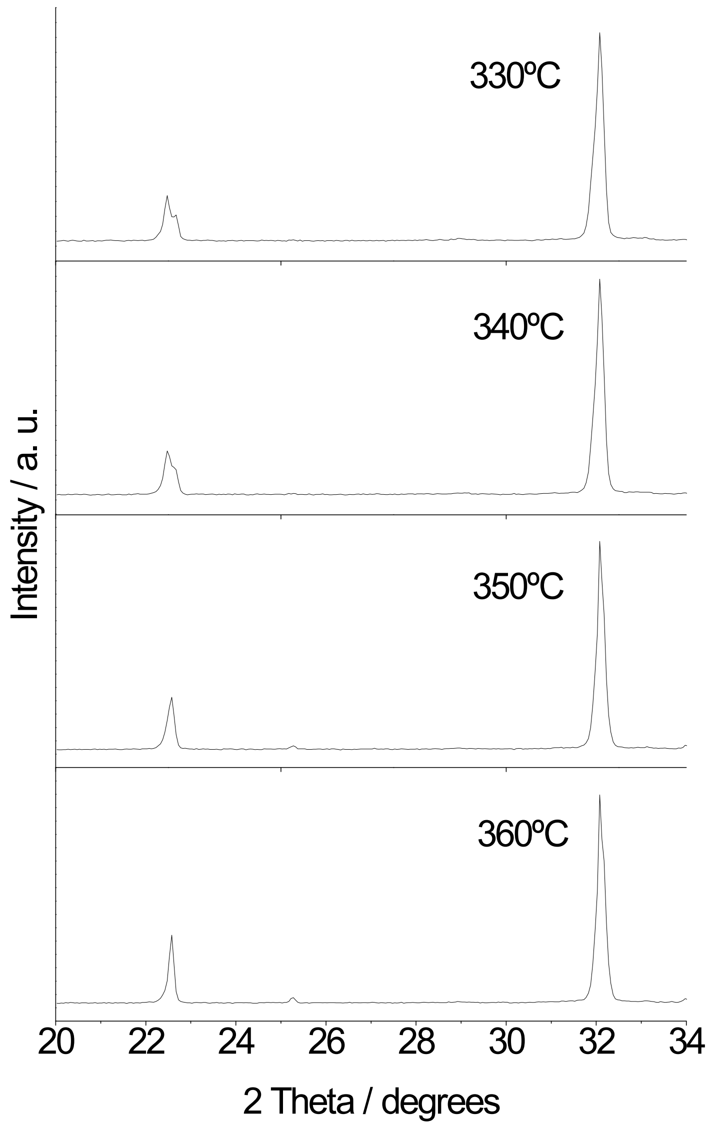

Figure S24. Detail of the XRD patterns measured at different temperatures (between 320ºC and 360ºC) for $Bi_{0.70}La_{0.30}FeO_3$. From 350ºC the double peak at about 22.5º transforms to a single peak and a new peak at 25.3º appears. The new phase can be indexed as Pnma, as was observed for compositions $x \leq 0.15$ above T_C. Other phase transitions at higher temperatures were not observed.

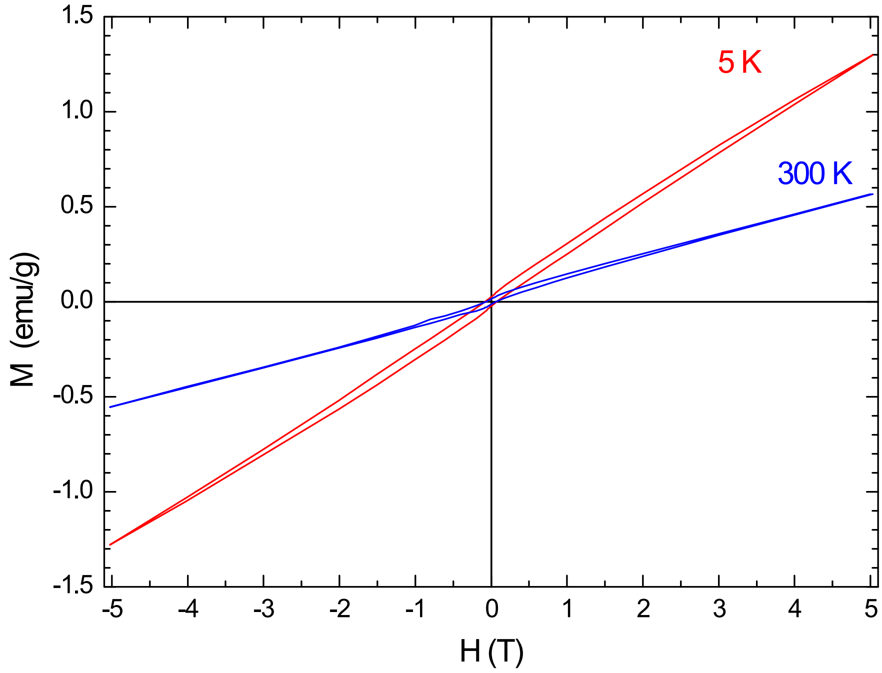

Figure S25. Magnetic field dependence of the magnetization at 5 K and 300 K for $BiFeO_3$ nanoparticles.

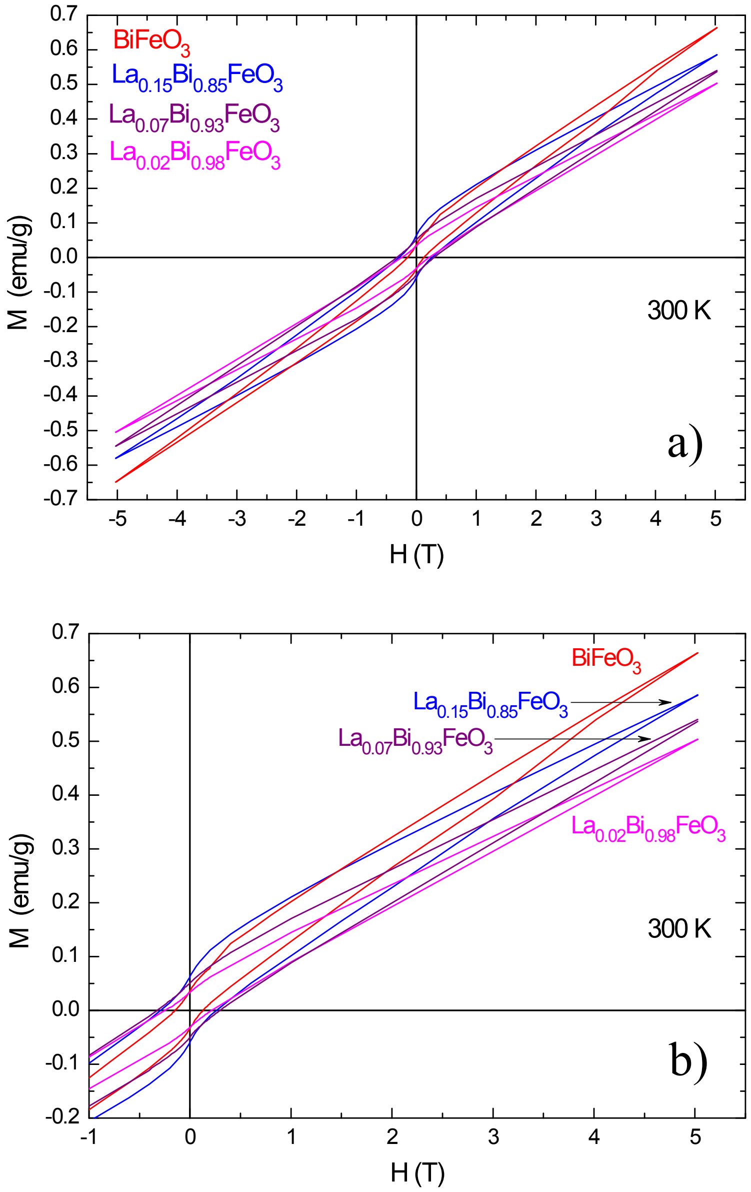

Figure S26. (a) Hysteresis loops obtained at 300 K for $Bi_{1-x}La_xFeO_3$ samples with x= 0, 0.02, 0.07 and 0.15. (b) Zoom of the hysteresis loops.